



# Detection of microplastics in human lung tissue using $\mu$ FTIR spectroscopy

Lauren C. Jenner<sup>a</sup>, Jeanette M. Rotchell<sup>b</sup>, Robert T. Bennett<sup>c</sup>, Michael Cowen<sup>c</sup>,  
Vasileios Tentzeris<sup>c</sup>, Laura R. Sadofsky<sup>a,\*</sup>

<sup>a</sup> Hull York Medical School, University of Hull, Hull HU6 7RX, United Kingdom

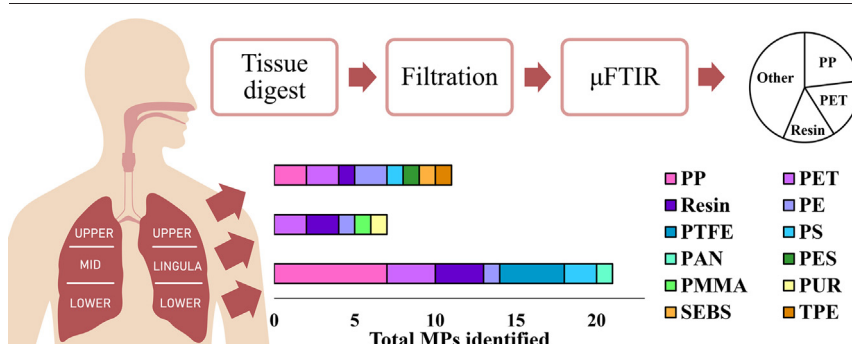
<sup>b</sup> Department of Biological and Marine Sciences, University of Hull, Hull HU6 7RX, United Kingdom

<sup>c</sup> Department of Cardiothoracic Surgery, Castle Hill Hospital, Cottingham HU16 5JQ, United Kingdom

## HIGHLIGHTS

- Microplastics were identified in all regions of the human lungs using  $\mu$ FTIR analysis.
- Polypropylene and polyethylene terephthalate fibres were the most abundant.
- The results support inhalation as a route of MP exposure.

## GRAPHICAL ABSTRACT



## ARTICLE INFO

Editor: Yolanda Pico

### Keywords:

Microplastic  
Lung  
Inhalation  
Human  
Atmospheric  
Airborne  
Air  
 $\mu$ FTIR

## ABSTRACT

Airborne microplastics (MPs) have been sampled globally, and their concentration is known to increase in areas of high human population and activity, especially indoors. Respiratory symptoms and disease following exposure to occupational levels of MPs within industry settings have also been reported. It remains to be seen whether MPs from the environment can be inhaled, deposited and accumulated within the human lungs. This study analysed digested human lung tissue samples ( $n = 13$ ) using  $\mu$ FTIR spectroscopy (size limitation of  $3 \mu\text{m}$ ) to detect and characterise any MPs present. In total, 39 MPs were identified within 11 of the 13 lung tissue samples with an average of  $1.42 \pm 1.50$  MP/g of tissue (expressed as  $0.69 \pm 0.84$  MP/g after background subtraction adjustments). The MP levels within tissue samples were significantly higher than those identified within combined procedural/laboratory blanks ( $n = 9$  MPs, with a mean  $\pm$  SD of  $0.53 \pm 1.07$ ,  $p = 0.001$ ). Of the MPs detected, 12 polymer types were identified with polypropylene, PP (23%), polyethylene terephthalate, PET (18%) and resin (15%) the most abundant. MPs (unadjusted) were identified within all regions of the lung categorised as upper ( $0.80 \pm 0.96$  MP/g), middle/lingular ( $0.41 \pm 0.37$  MP/g), and with significantly higher levels detected in the lower ( $3.12 \pm 1.30$  MP/g) region compared with the upper ( $p = 0.026$ ) and mid ( $p = 0.038$ ) lung regions. After subtracting blanks, these levels became  $0.23 \pm 0.28$ ,  $0.33 \pm 0.37$  and  $1.65 \pm 0.88$  MP/g respectively. The study demonstrates the highest level of contamination control and reports unadjusted values alongside different contamination adjustment techniques. These results support inhalation as a route of exposure for environmental MPs, and this characterisation of types and levels can now inform realistic conditions for laboratory exposure experiments, with the aim of determining health impacts.

**Abbreviations:** LOD, limit of detection; LOQ, limit of quantitation;  $\mu$ FTIR, micro Fourier Transform Infrared; MCT, mercury cadmium telluride; MP, microplastics between  $1 \mu\text{m}$  and  $5 \text{mm}$ ; NP, nanoplastics; PAN, polyacrylonitrile; PE, polyethylene; PES, polyester; PET, polyethylene terephthalate; PMMA, polymethylmethacrylate; PP, polypropylene; PS, polystyrene; PTFE, polytetrafluoroethylene; PUR, polyurethane; PVA, polyvinyl alcohol; ROS, reactive oxygen species; SEBS, styrene-ethylene-butylene co-polymer; TPE, thermoplastic elastomer.

\* Corresponding author.

E-mail address: [L.R.Sadofsky@hull.ac.uk](mailto:L.R.Sadofsky@hull.ac.uk) (L.R. Sadofsky).

<http://dx.doi.org/10.1016/j.scitotenv.2022.154907>

Received 23 December 2021; Received in revised form 25 March 2022; Accepted 25 March 2022

Available online 29 March 2022

## 1. Introduction

Microplastics (MPs), defined herein as plastic particles between 1  $\mu\text{m}$  and 5 mm (Hartmann et al., 2019), are present in all environmental compartments; from marine and freshwater bodies (GESAMP, 2015), to soil (Wang et al., 2019), food, drinking water (Danopoulos et al., 2020a; Danopoulos et al., 2020b), and air (Allen et al., 2019; Dris et al., 2017; Cai et al., 2017; Jenner et al., 2021). For the latter, suspended MP particles have been isolated from many atmospheric locations, including urbanised city centres (Cai et al., 2017; Wright et al., 2019a; Liu et al., 2019a), indoor households (Dris et al., 2017; Jenner et al., 2021; Vianello et al., 2019; Zhang et al., 2020), and remote outdoor regions (Allen et al., 2019). Previous work highlights that citizens are exposed to higher concentrations of MP within their homes (Jenner et al., 2021) or outdoor areas of high human activity (Jenner et al., 2022), and this results in ubiquitous and unavoidable human exposure (Prata et al., 2020). Consequently, there is an increasing concern regarding the hazards associated with MP ingestion, dermal contact, and inhalation (Prata et al., 2020).

Synthetic fibres have previously been observed within human lung tissue samples (Pauly et al., 1998), yet limited studies confirm the presence of MPs within the lungs alongside chemical analysis tools, such as  $\mu\text{Raman}$  and  $\mu\text{FTIR}$  spectroscopy (Amato-Lourenço et al., 2021). Reliance upon observational criteria alone to distinguish between MP and non-MPs, can lead to over and under-estimated MP counts, and a lack of information relating to polymer or additive type (Eriksen et al., 2013; Hidalgo-Ruz et al., 2012). The plausibility of MP inhalation has been highlighted (Prata, 2018; Wright and Kelly, 2017) and MPs with a width as small as 5  $\mu\text{m}$  have been reported within air samples (Wright et al., 2019a; Li et al., 2020). Upon environmental release, plastics are exposed to oxidation, mechanical stress and biological action, resulting in embrittlement and fragmentation, forming MPs, and eventually nanoplastics (NPs) (<1  $\mu\text{m}$ ), as well as release into the environment in their primary form (Hidalgo-Ruz et al., 2012).

Historical studies report respiratory symptoms and disease at an occupational level of exposure in synthetic textile, flock, and vinyl chloride workers (Prata, 2018), and as such, support inhalation as an exposure route for MPs. However, it remains unclear whether MPs can enter and remain in the lungs of the general population due to environmental exposure, rather than the chronic levels seen within industry settings. MPs are designed to be robust materials, unlikely to break down within the lungs (Law et al., 1990), potentially leading to accumulation over time depending on aerodynamic diameter and respiratory defences (Prata, 2018).

The mounting concern surrounding airborne MPs stems from the unknown polymer types, levels of exposure, and consequences of their inhalation. MP characteristics such as size, shape, vectored absorbed pollutants and pathogens, as well as plastic monomer or additive leaching, have been highlighted as potential promoters of cytotoxicity (Wright and Kelly, 2017). MPs are consistently identified within air samples, their concentration is highest indoors (Dris et al., 2017; Vianello et al., 2019; Zhang et al., 2020) and within highly populated areas (Cai et al., 2017), they are readily suspended at times of high human activity (Zhang et al., 2020) and are often small and fibrous (Liu et al., 2019a). Together, these concerns highlight the necessity for accurate tissue analysis to understand the potential for these synthetic polymers to penetrate the human respiratory system and cause harm.

This study aims to identify any MP particles present in digested human lung tissue samples, while also accounting for procedural and laboratory blank contamination. Any particles isolated from lung tissue have been chemically characterised using  $\mu\text{FTIR}$  spectroscopy (with a 3  $\mu\text{m}$  lower size limit of detection).

## 2. Material and methods

### 2.1. Human tissue acquisition

Excess human lung tissue was collected from thoracic surgical procedures at Castle Hill Hospital, Hull University Teaching Hospitals NHS

Trust, following NHS Research Ethics Committee and Health Research Authority approval (REC reference 12/SC/0474). Samples of peripheral human lung tissue were collected from upper, middle (left lingula) or lower lobe specimens following surgical resection for cancer or lung volume reduction surgery. Descriptions of the tissue origin were provided by the surgical team. Care was taken to avoid the tumour margins. Details of the donors smoking status, occupation and area of residence were unavailable for the researchers under the terms of the ethical approval obtained. Tissue samples were placed into empty glass containers with foil lids and immediately frozen ( $-80^{\circ}\text{C}$ ) until bulk analysis (two batches) was conducted. Lung tissue was obtained from 11 patients (numbered 1.1 to 11.1), with patients 1 and 2 providing two samples (numbered 1.2 and 2.2) from different lung positions ( $n = 13$ , total tissue mass = 55.41 g), resulting in a mean mass of  $4.26 \pm 3.87$  g (range 0.79–13.33 g). Patients mean age was  $63 \pm 13$  years (range 32–77), 5 females and 6 males (Table 1).

### 2.2. Lung tissue digestion and filtration

Thawed samples were exposed to a hydrogen peroxide (100 mL of 30%  $\text{H}_2\text{O}_2$ ) bath and rinsed alongside 'procedural blanks' ( $n = 4$ ) (Supplementary Fig. S1). Each tissue sample was transferred to a clean glass conical flask with a foil covering, and 100 mL of 30%  $\text{H}_2\text{O}_2$  added. The total mass of each individual tissue sample digested is detailed in Table 1. Flasks were placed in a shaking incubator at  $55^{\circ}\text{C}$  for approximately 11 days, 65 rpm, or until there was no visible tissue. After 5 days within the incubator, an additional 100 mL of 30%  $\text{H}_2\text{O}_2$  was added. The digest, adapted from previous studies investigating MPs within different environmental and tissue samples (Munno et al., 2018), ensures removal of organic particles while maintaining MP integrity (Allen et al., 2019; Munno et al., 2018). Samples were then filtered onto aluminium oxide filters (0.02  $\mu\text{m}$  Anodisc, Watford, U.K.) using a glass vacuum filtration system. These were stored in clean glass petri dishes, in the dark, before chemical composition analysis alongside laboratory blanks ( $n = 13$ ) (Supplementary Fig. S1).

### 2.3. Chemical characterisation of particles using $\mu\text{FTIR}$ analysis

Each tissue sample Anodisc filter was placed directly onto the  $\mu\text{FTIR}$  spectroscopy platform, and the length (largest side) and width (second largest side) recorded using the aperture height, width and angle size selection tool, available within the ThermoScientific Omnic Picta Nicolet iN10 microscopy software. Particles were then assigned to a shape category (fibre, film, fragment, foam, or sphere (Free et al., 2014)), whereby fibrous particles were characterised as having a length to width ratio  $> 3$  (Vianello et al., 2019).

$\mu\text{FTIR}$  spectroscopy analysis was conducted in liquid nitrogen cooled transmission mode (Nicolet iN10, ThermoFisher, Waltham MA, U.S.A.), without the aid of further accessories or crystals. The cooled mercury cadmium telluride (MCT) detector allowed for the analysis of particles accurately down to 3  $\mu\text{m}$  in size. The Nicolet iN10 microscope used is equipped with  $15 \times 0.7$  N.A. high efficiency objective and condenser. It has a colour CCD digital video camera with an independent reflection and transmission illuminations mounted, for capturing images of particles. This model has a standardised  $123\times$  magnification with the aperture settings used. No observational criteria (Hidalgo-Ruz et al., 2012) was applied to select specific particles for  $\mu\text{FTIR}$  analysis, to prevent bias. Using the aperture size selection tool, all particles upon the sample filter  $> 3 \mu\text{m}$  were included in the analysis process. For this study, the whole filter, containing the total digested tissue sample, was analysed.

A background reference spectrum was first recorded, using identical parameters to the particles undergoing analysis. A blank area of the Anodisc filter was chosen as the site for background collection before immediate analysis of the sample particles.  $\mu\text{FTIR}$  parameters were; spectral range of  $4000\text{--}1250 \text{ cm}^{-1}$ , high spectral resolution  $8 \text{ cm}^{-1}$ , scan number of 64. No smoothing, baseline correction or data transformation was attempted. Resulting sample spectra were compared to a combination of polymer libraries (Omnic Picta, Omnic Polymer Libraries), available with the Omnic

**Table 1**

Patient and tissue sample information alongside the number of MPs identified within samples by  $\mu$ FTIR spectroscopy. Polymer types and particle characteristics are included, and three different contamination adjustments to display results in units of MP/g of tissue. Abbreviations; PAN = polyacrylonitrile, PE = polyethylene, PES = polyester, PET = polyethylene terephthalate, PMMA = polymethylmethacrylate, PP = polypropylene, PS = polystyrene, PTFE = polytetrafluoroethylene, PUR = polyurethane, Resin = alkyd/epoxy/hydrocarbon, SEBS = styrene-ethylene-butylene co-polymer, TPE = thermoplastic elastomer. R = right lung, L = left lung, Low = lower region of the lung, mid = middle/lingular region of the lung, up = upper region of the lung.

ID	Sex	Lung region	Tissue (g)	MP total	MP polymer	Length, width ( $\mu$ m)	Shape	MP/g <sup>a</sup>	MP/g <sup>b</sup>	MP/g <sup>c</sup>
1.1	M	R, Low	2.02	8	PET PP PP PP PP PS PTFE PTFE	88, 10 55, 28 39, 18 420, 9 27, 10 89, 71 100, 29 92, 88	Fibre Fragment Fragment Fibre Fragment Fragment Fibre Film	3.96	2.97	1.94 based on PP only
1.2		R, Up	0.79	2	PP TPE	109, 18 66, 19	Fibre Fibre	2.53	0.00	
2.1	M	R, Low	0.80	3	PP PP PTFE	40, 22 144, 65 26, 20	Fragment Fragment Fragment	3.75	1.25	
2.2		L, Low	0.84	3	PS PTFE Resin	14, 14 96, 5 19, 13	Fragment Fibre Fragment	3.57	1.19	
3.1	M	R, Up	13.33	5	PE PE PET PP SEBS	224, 9 29, 17 202, 6 101, 17 83, 18	Fibre Fragment Fibre Fibre Film	0.38	0.23	
4.1	M	R, Up	1.53	2	PS Resin	60, 44 12, 9	Fragment Fragment	1.31	0.65	
5.1	F	L, Lin	1.37	0	none	none		0.00	0.00	
6.1	M	R, Mid	3.98	2	PE Resin	17, 10 20, 15	Fragment Fragment	0.50	0.25	
7.1	F	R, Up	8.29	1	PES	40, 22	Fragment	0.12	0.00	
8.1	F	L, Low	5.90	7	PAN PE PET PET PP Resin Resin PET PET PMMA PUR Resin	1112, 9 28, 20 443, 13 452, 12 160, 46 101, 9 261, 22 897, 10 2475, 12 96, 76 155, 16 14, 4	Fibre Fragment Fibre Fibre Fragment Fibre Fibre Fibre Fibre Fragment Fibre Fibre	1.19	1.19	
9.1	M	R, Mid	6.84	5	PET PET PMMA PUR Resin	897, 10 2475, 12 96, 76 155, 16 14, 4	Fibre Fibre Fragment Fibre Fibre	0.73	0.73	
10.1	F	R, Up	2.12	1	PET	275, 12	Fibre	0.47	0.47	
11.1	F	R, Up	7.60	0	none	none		0.00	0.00	
Mean $\pm$ SD								1.42 $\pm$ 1.5	0.69 $\pm$ 0.84	

<sup>a</sup> Total MPs detected with no account taken for MPs found in controls.

<sup>b</sup> Total MPs in sample minus total MPs identified in controls (regardless of polymer type) (Supplementary information).

<sup>c</sup> MP contamination levels after LoD/LoQ method (Cowger et al., 2020), if meeting the threshold (Supplementary information).

Picta software, and full spectral ranges were used with a match threshold of  $\geq 70\%$ . If particles were below the  $\geq 70\%$  match index threshold, three attempts were made to collect a successful match before moving on to the next particle undergoing analysis. Particles below  $\geq 70\%$  match, and particles not classified as a plastic were recorded but not included in the results presented (Cowger et al., 2020).

During  $\mu$ FTIR analysis, one 'laboratory blank' Anodisc filter was opened alongside every sample filter (Supplementary Fig. S1). A total of 13 lung tissue samples were analysed, plus 4 'procedural blanks', and 13 'laboratory blanks'. The total number of particles (MPs and others) identified was 296, whereby 225 (76%) of these were above the 70% hit quality index threshold. Only the MPs data is shown in the results. Identified PET and PES MP particles were reported separately within this study, using a high match ( $>70\%$ ) on a polymer database search to confirm their identities.

#### 2.4. Quality assurance and control measures to reduce and quantify background MP contamination

Strict control measures were adhered to, in order to quantify and characterise the nature of any unavoidable background contamination. Due to

the ubiquitous nature of MPs in the air, contamination upon the surface of lung tissue samples could be possible during the surgical procedure, where lung tissue was removed from live human subjects. While it was not possible to fully control the surgical environment, each tissue sample was dropped into a 100 mL 30% H<sub>2</sub>O<sub>2</sub> bath, re-sealed with foil and agitated for 2 min. In parallel, 'procedural blanks' (n = 4) were initiated. The tissue sample was removed, and the outer surface rinsed thoroughly with 100 mL 30% H<sub>2</sub>O<sub>2</sub> to remove any surface contamination, employing a method similar to extracting microplastics from whole biota (Brander et al., 2020). Analysis of solely the interior portion of the tissue was considered (Pauly et al., 1998) but was not applied with the aim of maintaining a larger tissue mass. Tissue samples were digested in two batches, with two procedural blanks, which mimicked the entire tissue processing steps but lacked the lung tissue sample, alongside each batch (Supplementary Fig. S1). Reagents were filtered and prepared in bulk for each batch. When conducting  $\mu$ FTIR analyses, a 'laboratory blank' filter (n = 13), placed in a glass sealed petri dish, was opened for the same duration as that for the tissue sample.

MPs found within 'procedural blanks' represent contamination from the laboratory reagents, equipment or fallout from the air during the transfer of samples. For each batch, the average procedural contamination was

calculated and assumed to be present within each of the tissue samples. MPs within 'laboratory blanks' represent contamination from atmospheric fall-out within the  $\mu$ FTIR laboratory room during particle characterisation. Procedural blank and laboratory blank results were combined to account for contamination at every step. No standardised protocols are currently adopted within the MPs research field to account for background contamination, so multiple contamination adjustments were applied in this study for comparison. These comprised two approaches: subtraction, routinely used in the MP research field, and a limit of detection (LOD) and limit of quantification (LOQ) technique (Horton et al., 2021) (Supplementary methods S1). Presenting raw data, subtraction, and LOD/LOQ adjusted results allows a comparison for each technique.

All  $H_2O_2$  and MilliQ water used were triple filtered using an all-glass vacuum filtration kit and 47 mm glass fibre grade 6 filters (GE Healthcare Life Sciences, Marlborough MA, U.S.A.). All glassware underwent thorough manual cleaning, before a dishwasher cycle using distilled water and then a manual three rinse wash with triple filtered MilliQ water. All equipment and reagents were always covered with foil lids and a small opening made when pouring. Additionally, when filtering digested samples, glassware and the sides of the filtration kit were rinsed three times with triple filtered MilliQ water to avoid sample particle loss. All work was conducted in a thoroughly cleaned fume cupboard with power 'off' and shield down to minimise unfiltered air flow (Wesch et al., 2017) and particle suspension (Wright et al., 2019b). Each tissue sample was processed individually to prevent cross contamination. Plastic equipment was avoided, glass petri dishes, a cotton laboratory coat, and a new set of nitrile gloves for each sample processing step were used. Tissue preparation and particle analysis was conducted at times of low activity, no room ventilation and  $\mu$ FTIR conducted in a single person room with no windows. Finally, work was conducted by a single researcher for standardisation. To ensure no particles were contaminating the Anodisc filters from the manufacturing process of the discs used, three random filters were chosen and observed under the  $\mu$ FTIR, in which no particles were present.

### 2.5. Statistical analysis

Tests for homogeneity and significance were performed on unadjusted MP values using SPSS. All data were determined not normally distributed with a Shapiro-Wilk test and either a Kruskal-Wallis or Mann-Whitney *U* test applied.

## 3. Results

### 3.1. MP abundance levels detected in human lung tissue samples

A total of 39 MPs were identified within 11 of the 13 human lung tissue samples. An overall unadjusted mean of  $3.00 \pm 2.55$  MPs per sample (range 0–8 MPs) were identified within human lung tissue samples, significantly higher levels ( $p = 0.001$ ) compared with  $0.53 \pm 1.07$  MP per sample detected in the combined blanks. When considering the mass of the tissue sample, without accounting for background contamination, a mean of  $1.42 \pm 1.50$  MP/g was detected (Table 1). After subtracting background contamination, this value becomes  $0.69 \pm 0.84$  MP/g (Table 1). An unadjusted mean of  $2.09 \pm 1.54$  MP/g of tissue was identified in male ( $n = 6$ ) and  $0.36 \pm 0.50$  MP/g of tissue in female ( $n = 5$ ) samples (adjusted to  $0.91 \pm 0.95$  MP/g and  $0.33 \pm 0.52$  MP/g respectively after subtracting background contamination). All male samples contained at least one MP particle, while two of the five female samples did not. The data was not normally distributed ( $p = 0.013$ ), and a Mann-Whitney *U* test revealed tissue samples from male patients had significantly higher levels of MP/g compared to females ( $p = 0.019$ ). A detailed description of the characterisation of background MP contamination (procedural and laboratory blanks) can be found in the supplemental information (Table S1).

### 3.2. MP particle characterisation from human lung tissue samples

A total of 12 polymer types were identified in the tissue samples, as detailed in Fig. 1A. PP (9, 23%) and PET (7, 18%) were the most abundant

(Fig. 1A). All MPs identified within tissue samples were fibre (19, 49%), fragment (17, 43%), or film (3, 8%), (Figs. 1B, 2). MP particles identified within the tissue samples had a mean particle length of  $223.10 \pm 436.16$   $\mu$ m (range 12–2475  $\mu$ m), and a mean particle width of  $22.21 \pm 20.32$   $\mu$ m (range 4–88  $\mu$ m) (Fig. 3A).

### 3.3. Characterisation of background MP contamination (procedural and laboratory blanks)

Considering all the blank samples, the mean background MP contamination rate detected was  $0.53 \pm 1.07$  MP per blank. Particles identified within 'procedural blanks' had a mean MP contamination rate of  $2.00 \pm 2.83$  MP per sample (range 0–4), for batch 1, whereby four MPs were identified on one filter: PE, PE/PP, PS, and a resin particle. No MPs were detected on the second filter for batch 1 (Table S1). No particles were identified within 'procedural blanks' from batch 2 of tissue samples on either of the two procedural blank filters (Table S1). Particles detected from 'laboratory blanks' ( $n = 13$ ) had an overall mean MP contamination rate of  $0.38 \pm 0.65$  MP per sample (range 0–2). This comprised one PET, PP, PS, PTFE and PVA particle from the 13 laboratory control filters (Table S1). The average length of MPs detected within the combined blank samples was  $105.22 \pm 92.82$   $\mu$ m (range 23–315  $\mu$ m), and an average width of  $34.44 \pm 22.61$   $\mu$ m (range 15–73  $\mu$ m). The shapes of MPs identified in the combined blank samples were either fragment (6, 67%), fibre (2, 22%), or film (1, 11%).

In addition to MP particles, non-MP 'natural polymer' particles were detected on the sample filters. Combining non-MP procedural and laboratory blank results  $9.04 \pm 4.84$  non-MP particles per sample were detected, comprised of cellulose and zein.

### 3.4. Background MP contamination adjustments

Using adjustments, to account for the combined procedural and blank contamination levels detected, decreases the level of MPs identified within tissue samples depending on the approach used (Table 1). After blank subtraction adjustments, the total MPs identified within tissue samples have a mean of  $0.69 \pm 0.84$  MP/g of tissue. Subtraction adjusted MP levels in human lung tissues were statistically significant compared to blank data (Mann-Whitney *U* test,  $p = 0.043$ ). Only one lung tissue sample (sample 1.1) fit the criteria for using a LOD and LOQ calculation, showing 1.94 MP/g, above the quantification threshold. The polymer type detected above this threshold was PP. MPs above the LOD, that can be detected within lung tissue samples, but not quantified, were PE, PET, PP, PTFE and resin.

### 3.5. MP distribution within human samples by lung region

MPs were identified within all regions of the lung (Fig. 4 and Table S2). An unadjusted mean of  $0.80 \pm 0.96$  MP/g was identified within the upper region (adjusted to  $0.23 \pm 0.28$  MP/g after background subtraction),  $0.41 \pm 0.37$  MP/g within the middle/lingular region (adjusted to  $0.33 \pm 0.37$  MP/g) and  $3.12 \pm 1.30$  MP/g within the lower region (adjusted to  $1.65 \pm 0.88$  MP/g). Data was not normally distributed ( $p = 0.013$ ) and a Kruskal-Wallis test showed that the number of MPs in the lower region were significantly higher than the middle/lingular ( $p = 0.038$ ) and the upper region ( $p = 0.026$ ). Within the upper region ( $n = 6$ , total mass = 33.66 g), 11 MPs were identified; PE (2, 18%), PET (2, 18%), PP (2, 18%), PES (1, 9%), PS (1, 9%), resin (1, 9%), SEBS (1, 9%), TPE (1, 9%). Within the middle/lingular region ( $n = 3$ , total tissue mass = 12.19 g), 7 MPs were identified; PET (2, 29%), resin (2, 29%), PE (1, 14%), PMMA (1, 14%), PUR (1, 14%). Within the lower region ( $n = 4$ , total tissue mass = 9.56 g), 21 MPs were identified; PP (7, 33%), PTFE (4, 19%), PET (3, 14%), Resin (3, 14%), PS (2, 10%), PAN (1, 5%), PE (1, 5%) (Fig. 4).

### 3.6. MP distribution within human lung tissue by individual patient

MPs were identified in 9 of the 11 patient lung samples. Multiple samples were taken from patient 1; 8 MPs in sample 1.1 and 2 MPs in sample



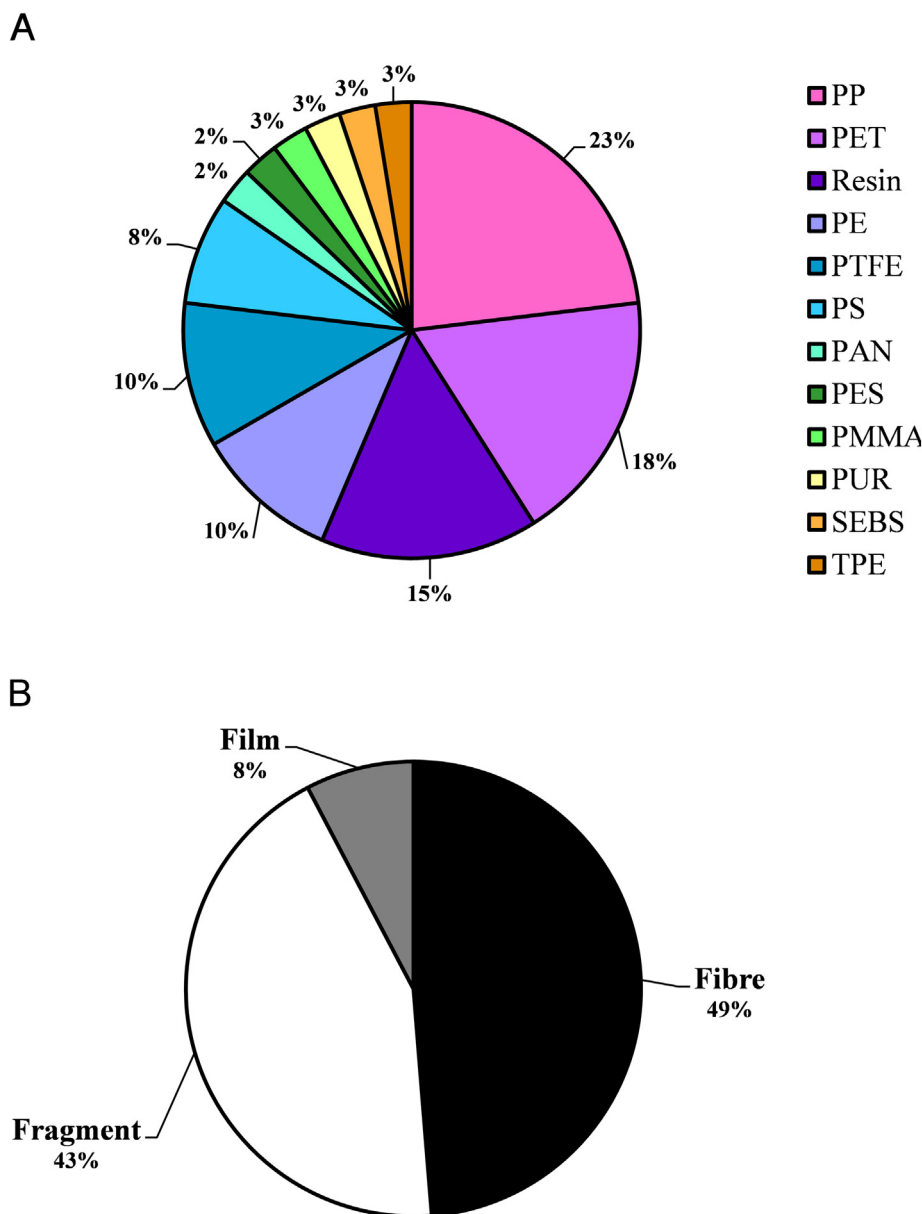


Fig. 1. Polymer types (A) and shapes (B) of the MPs identified within lung tissue samples.

1.2 (Fig. 5A). PP particles were identified within both samples (Fig. 5B). Multiple samples were also taken from patient 2; 3 MPs in sample 2.1 and 3 MPs in sample 2.2. PTFE particles were identified within both samples, while multiple polymers were only identified within one patient sample (Fig. 5B).

#### 4. Discussion

This report provides compelling evidence of MPs within human lung tissue samples, using a robust, best practice, background contamination regime combined with  $\mu$ FTIR chemical composition analysis to verify the particles present. The study also highlights the importance of including and evaluating contamination adjustments within MP research, while providing high levels of quality assurance and control.

In total, 39 MPs were identified within 11 of the 13 lung tissue samples, with an unadjusted average of  $1.42 \pm 1.50$  MP/g of tissue. By subtracting any MPs detected in the corresponding blanks, an adjusted average of  $0.69 \pm 0.84$  MP/g tissue sample is reported. The MP levels within tissue samples were significantly higher than those identified within combined

procedural/laboratory blanks. Of the MPs detected, 12 polymer types were identified with PP (23%), PET (18%), resin (15%), and PE (10%) the most abundant. It should be noted that the FTIR spectra for PET and PES (polyester) are similar and can be difficult to distinguish (Primpke et al., 2018; Veerasingam et al., 2021), however a high match of 70% was accepted to distinguish between the MP types within this study.

MPs were identified within all regions of the lung categorised as upper ( $0.80 \pm 0.96$  MP/g), middle/lingular ( $0.41 \pm 0.37$  MP/g), and lower ( $3.12 \pm 1.30$  MP/g) region. However, when a LOD and LOQ approach was applied, only one tissue sample fit the criteria, with only PP detected above the threshold levels at 1.94 MP/g (Table 1). It could be that most MPs identified were contamination, however the LOD LOQ could also be 'masking' legitimately identified MPs. The LOD LOQ adjustment approach dramatically reduced the level of quantifiable MPs identified within lung tissue samples. This quality control measure has the benefit of providing a threshold above that of a simple subtraction, allowing MPs to be reliably detected and quantified (Brander et al., 2020). Although it is an emerging technique within the MP field, it has the potential to account for polymer type as well as quantity and is commonly applied within analytical

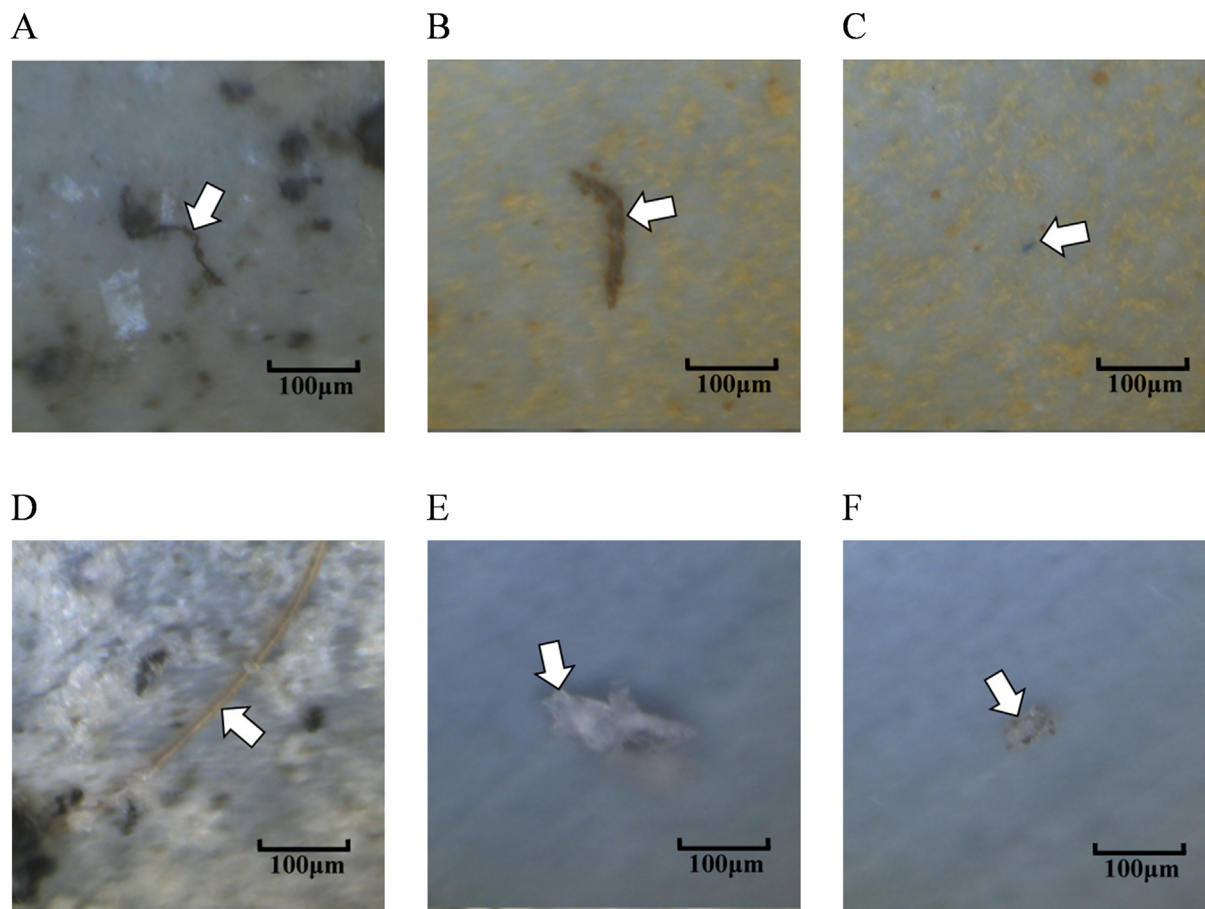


**Fig. 2.** Images of MPs identified from human lung tissue samples. A, B, C and D = (A = PET) (B = PUR) (C = Resin) (D = PAN). E and F = MPs identified within blanks. (E = PS) (F = PP). Corresponding spectra included in Fig. S2.

chemistry. However, samples containing low numbers of MPs, such as the human lung tissue samples reported here, commonly only have one MP particle per polymer type identified in a sample. It has been reported that when dealing with such low MP quantities within samples, the LOD LOQ technique will have more significant effects and lead to a “reduced capacity to report any MPs above the LOD or LOQ” (Horton et al., 2021). We therefore report our results in three ways; unadjusted, subtraction adjusted and LOD LOQ adjusted, but highlight the importance of the LOD LOQ technique for future studies in which MP abundance is not as low.

MPs have, to date, been detected in human samples from histological lung cancer samples (Pauly et al., 1998) and cadavers (Amato-Lourenço et al., 2021) as well as from human placenta (Ragusa et al., 2021). Our findings are consistent with an early study by Pauly et al. (1998) using microscopy under polarised light to identify fibres (though without chemical characterisation validation or rigorous contamination control measures), reporting presence of fibres in 83% of nonneoplastic lung specimens ( $n = 67/81$ ) and in 97% of malignant lung specimens ( $n = 32/33$ ) (Pauly et al., 1998). This study also reported that the fibres were distributed throughout all regions of the lung and were not confined to the large air spaces (Pauly et al., 1998). While no formal size range is given in this early study, they reported heterogeneity with respect to fibre length, width, surface morphology and colour, with  $>250\ \mu\text{m}$  length and  $\sim 50\ \mu\text{m}$  width (Pauly et al., 1998). Our findings are also in line with a recent publication by Amato-Lourenço et al. who also found PP to be amongst the most abundant plastics identified (Amato-Lourenço et al., 2021). In contrast to our study, Amato-Lourenço et al. showed that non-fibrous particles were the most abundant type of MP with sizes smaller than those seen in our study. This could partly be due to differing exposures to MP, our best

practice approach used to eliminate background contamination, or the methods used to detect and characterise samples, Raman vs.  $\mu\text{FTIR}$ . Although Raman spectroscopy has the advantage of a lower method detection limit ( $\sim 1\ \mu\text{m}$ ), which might explain the abundance of smaller particles identified in Amato-Lourenço study (Amato-Lourenço et al., 2021), it can be heavily influenced by fluorescence interference and does not detect the same polar peaks that  $\mu\text{FTIR}$  spectroscopy can. Additionally, Raman spectroscopy can UV degrade the particles being analysed, which could hinder potential future investigations. Thus, although both spectroscopic techniques complement each other,  $\mu\text{FTIR}$  has some advantages that benefit MP research (Silva et al., 2018).

Interestingly, tissue from male donors contained significantly higher levels of unadjusted MP ( $2.09 \pm 1.54\ \text{MP/g}$ ) compared to females ( $0.36 \pm 0.50\ \text{MP/g}$ ), with all samples from males containing MPs but two out of five samples from females showing no MPs. We hypothesise that this is due female airways being significantly smaller than the airways of males (Dominelli et al., 2018), although the relatively small sample size used herein dictates that more analyses be conducted to explore such differences further.

According to Donaldson et al. (1993), only particles with a physical diameter smaller than  $3\ \mu\text{m}$  can enter the alveolar region of the lung (Donaldson et al., 1993). The alveolar duct is reported in the literature as being  $\sim 540\ \mu\text{m}$  diameter and  $1410\ \mu\text{m}$  long (Horsfield et al., 1971). Particles of a size ranging from  $12$  to  $2475\ \mu\text{m}$  for length and  $4$ – $88\ \mu\text{m}$  for width were detected within lung samples in this study, in theory, too large to be present, yet present nonetheless.

While the fate of particles entering the lung, and their resulting biological effects in terms of inflammation responses, are well established for ultrafine particulates in the NP or  $\text{PM}_{10}$  size range (Oberdörster et al., 1994; Kreyling

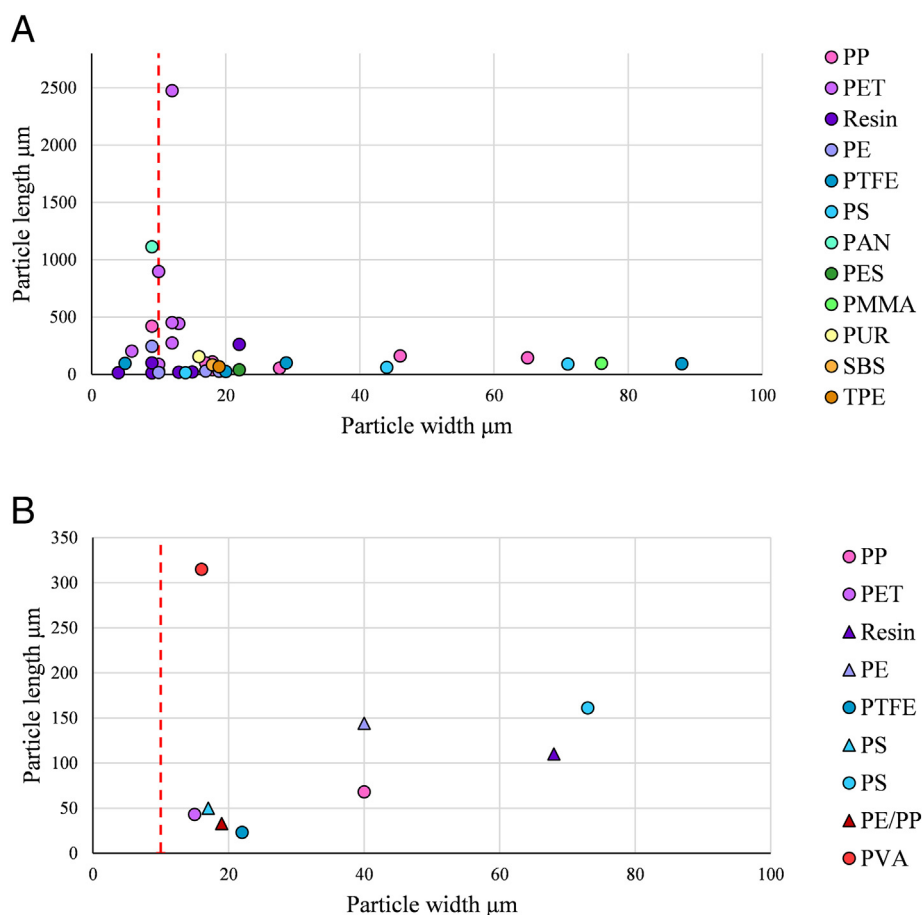


**Fig. 3.** Polymer size dimensions and type of each MP identified within (A) human lung tissue samples and (B) 'procedural blank' (triangles) and 'laboratory blank' (circles) samples. Red line represents the assumed inhalable size limit regardless of density.

et al., 2006), the corresponding information is currently unavailable for the MP size range of particles observed here, highlighting a serious gap in the knowledge. There are limited recent studies giving evidence of particle sizes and deposition in the lungs. It could be that there may be a pre-conceived assumption about the particle sizes which are inhalable and able to make it into the lower airway, but in this study, and others (Pauly et al., 1998; Amato-Lourenço et al., 2021) particles bigger than these are being reported, and therefore, it may be time to revisit these numbers and investigate what sizes can be inhaled. Interestingly, even after LOD and LOQ were applied, the PP identified in sample 1.1 was above the size limit which is generally thought of as inhalable.

12 MPs  $\leq 10 \mu\text{m}$  were identified within 7 of the 13 lung tissue samples, consisting of PET (3), resin (3), PE (2), PP (2), PTFE (1) and PAN (1) (Table 1). The smallest particle identified was  $14 \mu\text{m}$  in length and  $4 \mu\text{m}$  width (Fig. 2C), and identified as an 'alkyd resin', a synthetic thermoplastic used in protective coatings and paints (Polymer Properties Database, n.d.). No MPs  $\leq 10 \mu\text{m}$  were detected within blanks, surprising since the prevalence of MPs in the environment is known to increase with decreasing particle size (Allen et al., 2019; Dris et al., 2017; Cai et al., 2017), suggesting that the quality assurance measures undertaken eliminated these smaller particles from blanks. As these small MPs were consistently absent from blanks (Fig. 3B), it highlights the likelihood of the

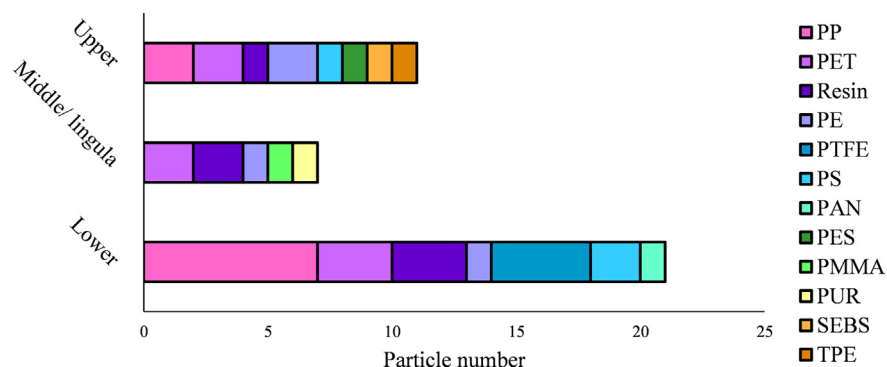


**Fig. 4.** Particle number (total MPs detected with no account taken for MPs found in controls) and polymer type of MPs identified within human lung tissue samples, assigned to their lung region.

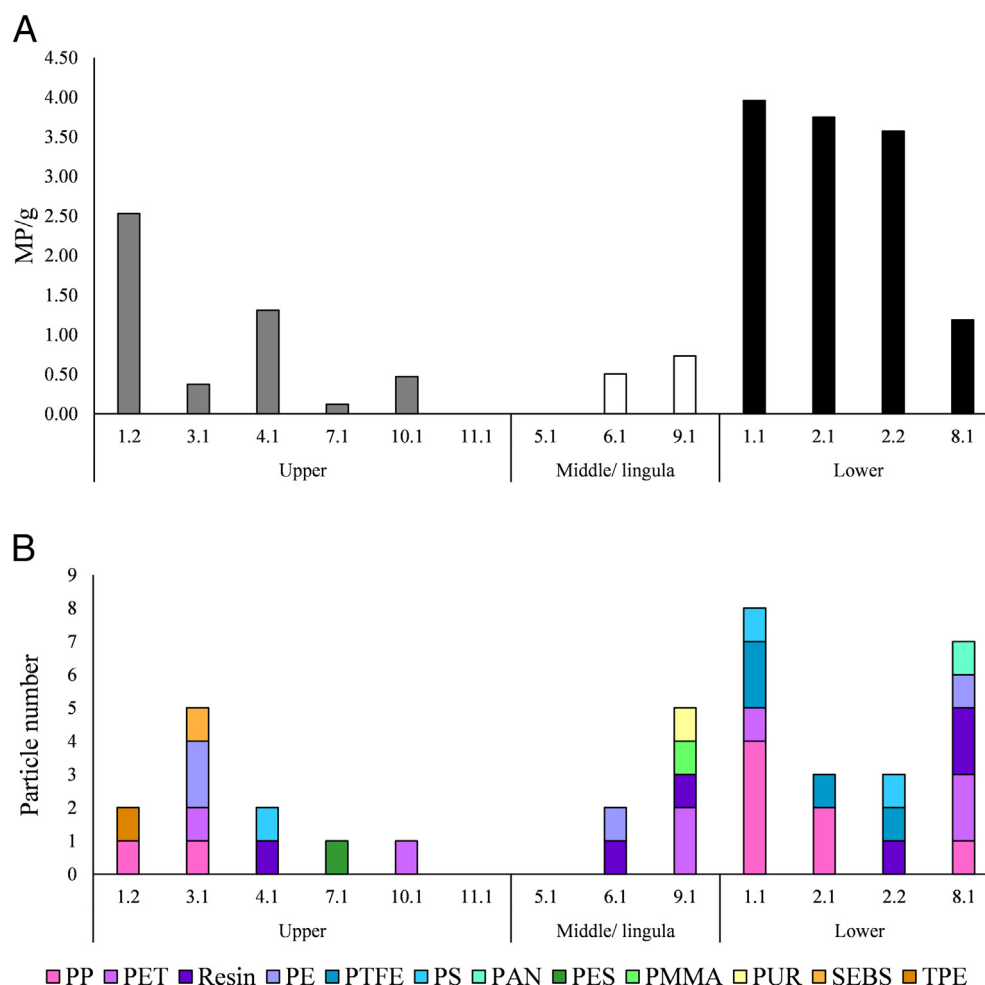


Fig. 5. Number (A) and type/quantity (B) of MPs detected in each lung region for individual patients.

smaller MPs being present within lung tissue rather than from background contamination sources.

The ubiquity of MPs within the environment, results in background contamination in any study, even after strict quality control measures are applied. Blanks, or controls, are run alongside sample analysis to document the levels and types of MPs contaminating samples, either by mimicking the sample processing steps ('procedural blank'), or by opening a clean filter during sample analysis ('laboratory blank'). Rarely are procedural and laboratory blanks both applied (Brander et al., 2020). It was hypothesised in the design of this study that if MPs were present within lung tissue samples, they would be present at low levels, especially considering the detection limit of chemical verification. Thus, the importance of combining multiple procedural and laboratory blanks, is highlighted. In this study the MP characteristics identified within blanks were distinct from those identified within lung tissue samples; the main polymer abundance, size range and shape varied (Fig. 3A, B). Human lung tissue samples were typically comprised of PP, PET and resin, with lengths ranging from 12 to 2475  $\mu\text{m}$  and widths from 4 to 88  $\mu\text{m}$ , and fibres being more prevalent than fragments. In contrast, MPs detected in the blanks were less abundant and comprised different particle characteristics. MPs were sized 23–315  $\mu\text{m}$  and 15–73  $\mu\text{m}$  for length and width, and fragments were more prevalent than fibres.

Within the MP literature, a standardised contamination adjustment technique has not been established. Therefore, this study opted to report concentrations in three commonly used ways; detailing blank results but making no adjustments (Zhang et al., 2020; Liu et al., 2019b), subtraction adjustments (Allen et al., 2019; Gaston et al., 2020) and LOD LOQ adjustments (Jenner et al., 2021; Horton et al., 2021). Using no contamination

adjustments,  $1.42 \pm 1.50$  MP/g of lung tissue was observed. While this method is common practice, it likely includes any contamination within the samples. The subtraction adjustment decreases the lung tissue MP final mean value to  $0.69 \pm 0.84$  MP/g and accounts for any potential background contamination but is not specific in terms of taking into account particle characteristics. The LOD LOQ adjustment approach dramatically reduces the levels of MPs identified within the study to  $0.15 \pm 0.54$  MP/g using a polymer specific approach, but could be seen to 'mask' low levels of MPs. Ultimately this study highlights the need for data adjustments to account for background contamination, but alongside an evaluation into which adjustment is the best approach. Irrespective of the adjustments, low levels of MPs are present within lung tissue samples, providing evidence to support MP inhalation as a route of exposure to humans.

Airborne MPs are globally ubiquitous and especially prevalent indoors where humans spend many hours a day, such as the home (Dris et al., 2017; Jenner et al., 2021; Vianello et al., 2019; Zhang et al., 2020) and the office (Dris et al., 2017; Zhang et al., 2020). Humans are thus continuously exposed to atmospheric MPs, with inhalation estimates ranging from 6 to 272 MP/day (Vianello et al., 2019; Prata, 2018; Domenech and Marcos, 2021). It is the smallest and least dense MP and NP particles that are the most cause for concern regarding respiratory health, as these MPs are most likely to deposit within the lungs based on aerodynamic diameter (Prata, 2018). In contrast to NPs, MP particles in the full micro-size range (10  $\mu\text{m}$ –5 mm) have yet to be considered in terms of health implications and potential impacts, perhaps not having been a priority compared with the smaller, ultrafine particles. The results herein indicate that the larger micro-size range is detected within human lung samples, suggesting that these have been overlooked (as being considered too large to enter



lungs). MPs, like all macroplastics, are designed to be resilient, with the addition of dyes, and additives that dictate their properties (GESAMP, 2015). It had previously been suggested that inhaled MPs are likely to bio-persist and possibly accumulate within a lung environment (Wright and Kelly, 2017), showing resilience to degradation by synthetic extracellular lung fluid after 180 days (Law et al., 1990). After deposition within the lung, mechanisms of toxicity are unknown but particle properties such as small size, density, concentration, shape, monomer type, chemical leachates and environmental adsorbents (e.g. bacteria, heavy metals and polyaromatic hydrocarbons) have all been suggested as potential contributors to cytotoxicity (Prata, 2018; Wright and Kelly, 2017). Inflammation (Porter et al., 1999), ROS and oxidative stress (Schirizzi et al., 2017), physical damage from particle shape, frustrated phagocytosis (Donaldson et al., 1993), are currently suggested cellular responses to MP exposure.

In summary, this study is the first to report MPs within human lung tissue samples, using  $\mu$ FTIR spectroscopy. The abundance of MPs within samples, significantly above that of blanks, supports human inhalation as a route of environmental exposure. MPs with dimensions as small as 4  $\mu$ m but also, surprisingly, >2 mm were identified within all lung region samples, with the majority being fibrous and fragmented. The knowledge that MPs are present in human lung tissues can now direct future cytotoxicity research to investigate any health implications associated with MP inhalation.

### CRedit authorship contribution statement

**Lauren C. Jenner:** Conceptualization, Investigation, Methodology, Formal analysis, Writing – original draft, Writing – review & editing, Visualization. **Jeanette M. Rotchell:** Conceptualization, Formal analysis, Writing – original draft, Writing – review & editing, Supervision. **Robert T. Bennett:** Resources, Writing – review & editing. **Michael Cowen:** Resources, Writing – review & editing. **Vasileios Tentzeris:** Resources, Writing – review & editing. **Laura R. Sadofsky:** Conceptualization, Formal analysis, Writing – original draft, Writing – review & editing, Supervision.

### Declaration of competing interest

The authors declare that they have no known competing financial interests or personal relationships that could have appeared to influence the work reported in this paper.

### Acknowledgements

This research did not receive any specific grant from funding agencies in the public, commercial, or not-for-profit sectors. It was funded by a PhD scholarship in the “Human Health and Emerging Environmental Contaminants” cluster funded by the University of Hull.

### Appendix A. Supplementary data

Supplementary data to this article can be found online at <https://doi.org/10.1016/j.scitotenv.2022.154907>.

### References

- Allen, S., Allen, D., Phoenix, V., et al., 2019. Atmospheric transport and deposition of microplastics in a remote mountain catchment. *Nat. Geosci.* 12, 339–344.
- Amato-Lourenço, L.F., Carvalho-Oliveira, R., Júnior, G.R., et al., 2021. Presence of airborne microplastics in human lung tissue. *J. Hazard. Mater.* 416, 126124.
- Brander, S.M., Renick, V.C., Foley, M.M., et al., 2020. Sampling and quality assurance and quality control: a guide for scientists investigating the occurrence of microplastics across matrices. *Appl. Spectrosc.* 74, 1099–1125.
- Cai, L., Wang, J., Peng, J., et al., 2017. Characteristic of microplastics in the atmospheric fall-out from Dongguan City, China: preliminary research and first evidence. *Environ. Sci. Pollut. Res.* 24, 24928–24935.
- Cowger, W., Booth, A.M., Hamilton, B.M., et al., 2020. Reporting guidelines to increase the reproducibility and comparability of research on microplastics. *Appl. Spectrosc.* 74, 1066–1077.
- Danopoulos, E., Twiddy, M., Rotchell, J.M., 2020. Microplastic contamination of drinking water: a systematic review. *PLoS ONE* 15, e0236838.
- Danopoulos, E., Jenner, L.C., Twiddy, M., et al., 2020. Microplastic contamination of seafood intended for human consumption: a systematic review and meta-analysis. *Environ. Health Perspect.* 128, 126002-1–126002-32.
- Domenech, J., Marcos, R., 2021. Pathways of human exposure to microplastics, and estimation of the total burden. *Curr. Opin. Food Sci.* 39, 144–151.
- Dominelli, P.B., Ripoll, J.G., Cross, T.J., Baker, S.E., Wiggins, C.C., Welch, B.T., Joyner, M.J., 2018. Sex differences in large conducting airway anatomy. *J. Appl. Physiol.* 125, 960–965.
- Donaldson, K., Brown, R.C., Brown, G.M., 1993. Respirable industrial fibres: mechanisms of pathogenicity. *Thorax* 48, 390–395.
- Dris, R., Gasperi, J., Mirande, C., et al., 2017. A first overview of textile fibers, including microplastics, in indoor and outdoor environments. *Environ. Pollut.* 221, 453–458.
- Eriksen, M., Mason, S., Wilson, S., et al., 2013. Microplastic pollution in the surface waters of the Laurentian Great Lakes. *Mar. Pollut. Bull.* 77, 177–182.
- Free, C.M., Jensen, O.P., Mason, S.A., et al., 2014. High-levels of microplastic pollution in a large, remote, mountain lake. *Mar. Pollut. Bull.* 85, 156–163.
- Gaston, E., Woo, M., Steele, C., et al., 2020. Microplastics differ between indoor and outdoor air masses: insights from multiple microscopy methodologies. *Appl. Spectrosc.* 74, 1079–1098.
- GESAMP, 2015. Sources, Fate and Effects of Microplastics in the Marine Environment: A Global Assessment. 40. The Joint Group of Experts on Scientific Aspects of Marine Environmental Protection, Working Group, London UK.
- Hartmann, N.B., Hüffer, T., Thompson, R.C., et al., 2019. Are we speaking the same language? Recommendations for a definition and categorization framework for plastic debris. *Environ. Sci. Technol.* 53, 1039–1047.
- Hidalgo-Ruz, V., Gutov, L., Thompson, R.C., et al., 2012. Microplastics in the marine environment: a review of the methods used for identification and quantification. *Environ. Sci. Technol.* 46, 3060–3075.
- Horsfield, K., Dart, G., Olson, D.E., et al., 1971. Models of the human bronchial tree. *J. Appl. Physiol.* 31, 207–217.
- Horton, A.A., Cross, R.K., Read, D.S., et al., 2021. Semi-automated analysis of microplastics in complex wastewater samples. *Environ. Pollut.* 268, 115841.
- Jenner, L.C., Sadofsky, L.R., Danopoulos, E., et al., 2021. Household indoor microplastics within the Humber region (United Kingdom): quantification and chemical characterisation of particles present. *Atmos. Environ.* 259, 118512.
- Jenner, L.C., Sadofsky, L.R., Danopoulos, E., Chapman, E., White, D., Jenkins, R.L., et al., 2022. Outdoor atmospheric microplastics within the Humber region (United Kingdom): quantification and chemical characterisation of deposited particles present. *Atmosphere* 13, 265.
- Kreyling, W.G., Semmler-Behnke, M., Möller, W., 2006. Ultrafine particle-lung interactions: does size matter? *J. Aerosol Med.* 19, 74–83.
- Law, B.D., Bunn, W.B., Hesterberg, T.W., 1990. Solubility of polymeric organic fibers and manmade vitreous fibers in gambles solution. *Inhal. Toxicol.* 2, 321–339.
- Li, Y., Shao, L., Wang, W., et al., 2020. Airborne fiber particles: types, size and concentration observed in Beijing. *Sci. Total Environ.* 705, 135967.
- Liu, K., Wang, X., Fang, T., et al., 2019. Source and potential risk assessment of suspended atmospheric microplastics in Shanghai. *Sci. Total Environ.* 675, 462–471.
- Liu, K., Wang, X., Wei, N., et al., 2019. Accurate quantification and transport estimation of suspended atmospheric microplastics in megacities: implications for human health. *Environ. Int.* 132, 105127.
- Munno, K., Helm, P.A., Jackson, D.A., et al., 2018. Impacts of temperature and selected chemical digestion methods on microplastic particles. *Environ. Toxicol. Chem.* 37, 91–98.
- Oberdorster, G., Ferin, J., Lehnert, B.E., 1994. Correlation between particle size, in vivo particle persistence, and lung injury. *Environ. Health Perspect.* 102, 173–179.
- Pauly, J.L., Stegmeier, S.J., Allaart, H.A., et al., 1998. Inhaled cellulosic and plastic fibers found in human lung tissue. *Cancer Epidemiol. Biomark. Prev.* 7, 419–428.
- Polymer Properties Database. Alkyd Resins <https://polymerdatabase.com/polymer%20classes/Alkyd%20Resin.html> Date last accessed: Jul 2021.
- Porter, D.W., Castranova, V., Robinson, V.A., et al., 1999. Acute inflammatory reaction in rats after intratracheal instillation of material collected from a nylon flocking plant. *J. Toxicol. Environ. Health Part A* 57, 25–45.
- Prata, J.C., 2018. Airborne microplastics: consequences to human health? *Environ. Pollut.* 234, 115–126.
- Prata, J.C., da Costa, J.P., Lopes, I., et al., 2020. Environmental exposure to microplastics: an overview on possible human health effects. *Sci. Total Environ.* 702, 134455.
- Primpke, S., Wirth, M., Lorenz, C., Gerds, G., 2018. Reference database design for the automated analysis of microplastic samples based on Fourier transform infrared (FTIR). *Anal. Bioanal. Chem.* 410, 5131–5141.
- Ragusa, A., Svelato, A., Santacroce, C., et al., 2021. Plasticenta: first evidence of microplastics in human placenta. *Environ. Int.* 146, 106274.
- Schirizzi, G.F., Pérez-Pomeda, I., Sanchis, J., et al., 2017. Cytotoxic effects of commonly used nanomaterials and microplastics on cerebral and epithelial human cells. *Environ. Res.* 159, 579–587.
- Silva, A.B., Bastos, A.S., Justino, C.I.L., da Costa, J.P., Duarte, A.C., Rocha-Santos, T.A.P., 2018. Microplastics in the environment: challenges in analytical chemistry - a review. *Anal. Chim. Acta* 1017, 1–19.
- Veerasingam, S., Ranjani, M., Venkatachalapathy, R., et al., 2021. Contributions of Fourier transform infrared spectroscopy in microplastic pollution research: a review. *Crit. Rev. Environ.* 51, 2681–2743.
- Vianello, A., Jensen, R., Liu, L., et al., 2019. Simulating human exposure to indoor airborne microplastics using a breathing thermal manikin. *Sci. Rep.* 9, 8670.

- Wang, J., Liu, X., Li, Y., et al., 2019. Microplastics as contaminants in the soil environment: a mini-review. *Sci. Total Environ.* 691, 848–857.
- Wesch, C., Elert, A.M., Wörner, M., et al., 2017. Assuring quality in microplastic monitoring: about the value of clean-air devices as essentials for verified data. *Sci. Rep.* 7, 1–8.
- Wright, S., Levermore, J., Kelly, F., 2019. Raman spectral imaging for the detection of inhalable microplastics in ambient particulate matter samples. *Environ. Sci. Technol.* 53, 8947–8956.
- Wright, S.L., Kelly, F.J., 2017. Plastic and human health: a micro issue? *Environ. Sci. Technol.* 51, 6634–6647.
- Wright, S.L., Ulke, J., Font, A., et al., 2019. Atmospheric microplastic deposition in an urban environment and an evaluation of transport. *Environ. Int.* 136, 105411.
- Zhang, Q., Zhao, Y., Du, F., et al., 2020. Microplastic fallout in different indoor environments. *Environ. Sci. Technol.* 54, 6530–6539.